Available online at www.sciencedirect.com
SCIENCE DIRECT®
Materials Chemistry and Physics 82 (2003) 5–15
MATERIALS CHEMISTRY AND PHYSICS
www.elsevier.com/locate/matchemphys

Electroanalytical studies on sol–gel derived $LiNi_{0.8}Co_{0.2}O_2$

G. Ting-Kuo Fey*, Zai-Xian Weng, Jian-Ging Chen, T. Prem Kumar[1]

Department of Chemical and Materials Engineering, National Central University, Chung-Li 32054, Taiwan ROC

Received 24 August 2002; received in revised form 29 September 2002; accepted 30 October 2002

Abstract

The electrochemical behavior of $LiNi_{0.8}Co_{0.2}O_2$, synthesized by a sol–gel method with maleic acid as a chelating agent, was investigated using galvanostatic charge–discharge cycling and electrochemical impedance spectroscopy. Unimolar solutions of $LiPF_6$ in mixed carbonate solvents such as EC:DEC, DEC:DMC, PC:DMC and EC:DEC:DMC were used as the electrolytes. The impedance response was found to be dependent on the extent of intercalation and deintercalation, although it was independent of the electrolyte composition. However, the charge–discharge behavior of the cathode material was found to be dependent on the electrolyte composition. Cells with 1 M $LiPF_6$ in EC:DEC gave the highest capacity. With this electrolyte, the first-cycle discharge capacity was 187 mAh g^{-1}. The first-cycle capacities obtained with the other electrolytes were lower, between 174 and 182 mAh g^{-1}. The impedance parameters of the system at different levels of intercalation and deintercalation were derived using equivalent circuit models.

Keywords: Cathode materials; Non-aqueous electrolytes; Electrochemical impedance spectroscopy; Lithium batteries

1. Introduction

Lithiated nickel oxide of the α-$NaFeO_2$ structure [1] with ABCABC oxygen stacking is a promising 4 V cathode material for lithium batteries. However, the preparation of phase-pure $LiNiO_2$ is a major hurdle to its application in commercial lithium cells. Preparations invariably end up in disordered $Li_{1-x}Ni_{1+x}O_2$ ($x > 0$) stoichiometries with excess nickel ions positioned in the lithium planes [2,3]. The similarity between their sizes (0.69 Å for the Ni^{2+} and 0.72 Å for the Li^+ ions) favors the formation of a three-dimensional rock salt structure over the two-dimensional layered structure [4,5]. The nickel ions in the lithium planes frustrate the layered structure and hinder the easy movement of lithium ions during the charge and discharge processes. Furthermore, the material shows a phase transition during the lithium deintercalation process [6,7] resulting in capacity fade and irreversible capacity loss. Substituting part of the nickel with a trivalent cation such as aluminum [8], iron [9] or titanium [10,11] has been attempted by several groups in order to restrain the phase transition. However, substitution with trivalent cobalt ions has been the most extensively studied. In fact, the products obtained by such substitutions are iso-structural solid solutions for all values of y in the general formula $LiNi_{1-y}Co_yO_2$, and have been widely recognized as structurally more stable cathode materials [12–15]. According to Delmas et al. [16] and Aragane et al. [17], the solid solution of the composition $LiNi_{0.8}Co_{0.2}O_2$ is a potential next-generation cathode material. However, Aragane et al. [17] point out that, given the vast disparity in the electrochemical properties of such solid solutions prepared by different routes, much care needs to be exercised in the synthesis and processing of the material.

The compatibility of the electrolyte with the cathode-active materials has a definite influence on the electrochemical response of the system. Fan and Fedkiw [18], who studied compacted cathodes ($LiCoO_2$, $LiNiO_2$ and $LiMn_2O_4$) by electrochemical impedance spectroscopy, found that the impedance behavior prior to cycling can be an indicator of cell performance. Levi et al. [19], who used slow scan cyclic voltammetry, potentiostatic intermittent titration and impedance studies to study $LiCoO_2$, found that the lithium insertion process has a serial character involving migration through surface films, charge-transfer, solid-state diffusion, etc. In the first report of its kind, Dokko et al. [20] used the impedance technique on a micrometer-sized single-particle $LiCoO_2$ to elucidate kinetic parameters. Electroanalytical

* Corresponding author. Tel.: +886-3-422-7151-4206/886-3-425-7325; fax: +886-3-425-7325.
E-mail address: gfey@cc.ncu.edu.tw (G.T.-K. Fey).
[1] On deputation from Central Electrochemical Research Institute, Karaikudi 630006, TN, India.

0254-0584/$ – see front matter © 2003 Elsevier B.V. All rights reserved.
doi:10.1016/S0254-0584(03)00225-6

behavior of $LiNi_{1-y}Co_yO_2$ phases has also been studied. For example, Croce et al. [21] interpreted their impedance data on the basis of electronic and ionic transport properties. Levi et al. [22], from their cyclic voltammetric and impedance studies on a commercial sample of $LiNi_{0.8}Co_{0.2}O_2$, found that the material underwent a somewhat rapid degradation in capacity at high anodic polarizations. Nobili et al. [23,24] found that at the initial stages of the deintercalation process the materials underwent a semiconductor-to-metal transition. The impedance response of $LiNiO_2$ in different organic electrolytes was also studied [25,26]. The capacity was dependent on the electrolyte salt and partly consistent with the ionic conductivity of the electrolyte solution [25,26].

In this paper, we report our results on the electrochemical impedance response of $LiNi_{0.8}Co_{0.2}O_2$, synthesized by a sol–gel route with maleic acid as the chelating agent, in $LiPF_6$-based electrolytes containing different mixed carbonate solvents. Impedance spectra were interpreted using equivalent circuit models. The capacity and cyclability of the sol–gel derived products were also determined in the various electrolytes.

2. Experimental

The synthesis of $LiNi_{0.8}Co_{0.2}O_2$ was carried out by a sol–gel method using maleic acid as a chelating agent [27]. The charge–discharge properties were studied with 2032-type coin cells with $LiNi_{0.8}Co_{0.2}O_2$ as the cathode and lithium metal (Foote Mineral) as the anode. The electrolytes used were 1 M $LiPF_6$ in (1) 50:50 (v/v) EC:DEC (Tomiyama Chemicals), (2) 50:50 (v/v) DEC:DMC (Ferro Chemicals), (3) 50:50 (v/v) PC:DMC (Tonyan Chemicals), and (4) 35:15:50 (v/v) EC:DEC:DMC (Ferro Chemicals). Celgard 2400 was used as the separator. The cathodes were fabricated by blade-coating an 85:10:5 slurry of $LiNi_{0.8}Co_{0.2}O_2$, carbon black and PVdF in NMP on to an aluminum foil, drying overnight at 120 °C in an oven, roller-pressing and punching out circular discs. The cell assembly was done in an argon-filled glove box (VAC MO 40-1), which contained less than 2 ppm oxygen and moisture. The cells were cycled at a 0.1 °C rate between 3.0 and 4.2 V in a constant current mode on a Maccor Series 4000 multi-channel battery tester.

The 2032-type coin cells, galvanostatically charged and discharged to various depths, were used for the impedance studies. The impedance spectra were recorded using a Schlumberger 1286 electrochemical interface and frequency response analyzer (Model 1255), driven by Corrware software (Scribner Associates). The frequency range was 65 kHz to 0.001 Hz and the amplitude of the perturbation signal was 20 mV. The impedance spectra were analyzed with Z-view software (Scribner Associates). Equivalent circuit models were proposed in order to evaluate the impedance parameters at different values of x in $Li_xNi_{0.8}Co_{0.2}O_2$.

3. Results and discussion

3.1. Charge–discharge studies

The charge–discharge curves of $LiNi_{0.8}Co_{0.2}O_2$ in different organic electrolytes are shown in Fig. 1. The charge–discharge behavior was found to be the best for the system with 1 M $LiPF_6$ in 50:50 EC:DEC as the electrolyte, with first- and tenth-cycle discharge capacities of 187 and 182 mAh g^{-1}, respectively. The corresponding values reported in our earlier paper [27] were 190 and 183 mAh g^{-1}, respectively. However, the small variations in the capacity of the products prepared in the two batches are within experimental error. The charge–discharge behavior of the product was also studied in the other electrolyte compositions. The first- and tenth-cycle discharge capacities were 182 and 177 mAh g^{-1} (DEC:DMC), 179 and 174 mAh g^{-1} (PC:DMC) and 174 and 168 mAh g^{-1} (EC:DEC:DMC). The first-cycle discharge capacities obtained with the different mixed solvents were in the order: EC : DEC > DEC : DMC > PC : DMC > EC : DEC : DMC. However, the capacity fade over 10 cycles were in the order EC:DEC:DMC (3.4%) > PC:DMC (2.8%) ≈ DEC:DMC (2.7%) ≈ EC:DEC (2.7%). It can be seen that all the electrolytes that contained DMC provided reduced capacities for the cathode material. Apparently, DMC as an electrolyte constituent seems to limit the utilization level of the cathode active material. Other possible electrolyte compositions without DMC were not studied because such commercial samples were not available.

It should be noted that the salt in all the electrolytes was $LiPF_6$. Since the electrolyte does not participate in the cell reaction, any contribution to capacity from the electrolytes could come from the mobility of lithium ions in the electrolyte and lithium diffusion characteristics due to changes in the composition of the solid electrolyte interface. Both the cyclic esters, PC and EC, have high dielectric constants favoring dissolution of the salt, but their high viscosities impede ionic mobility. On the other hand, the low viscosity linear alkyl carbonates provide a medium for ionic transport. All the electrolytes have conductivity values in the 10^{-3} to 10^{-2} S cm^{-1} range. Morita et al. [26], who studied the discharge behavior of $LiNiO_2$ and $LiMn_2O_4$ in various mixed carbonate electrolytes, showed that the discharge capacities were generally consistent with the conductivity of the electrolyte. The electrolytes apparently have an effect on the utilization of the electrode material because the mass transfer processes in the porous electrode structure is influenced by electrolyte conductivity. Although it is recognized that the nature of the electrolyte plays an important role in the discharge behavior of oxide electrodes [28–30], no explanation of the role played by the electrolyte has emerged yet. However, Morita et al. [25,26] showed that electrolyte solutions that had lower oxide/electrolyte interfacial resistances gave higher discharge capacities.

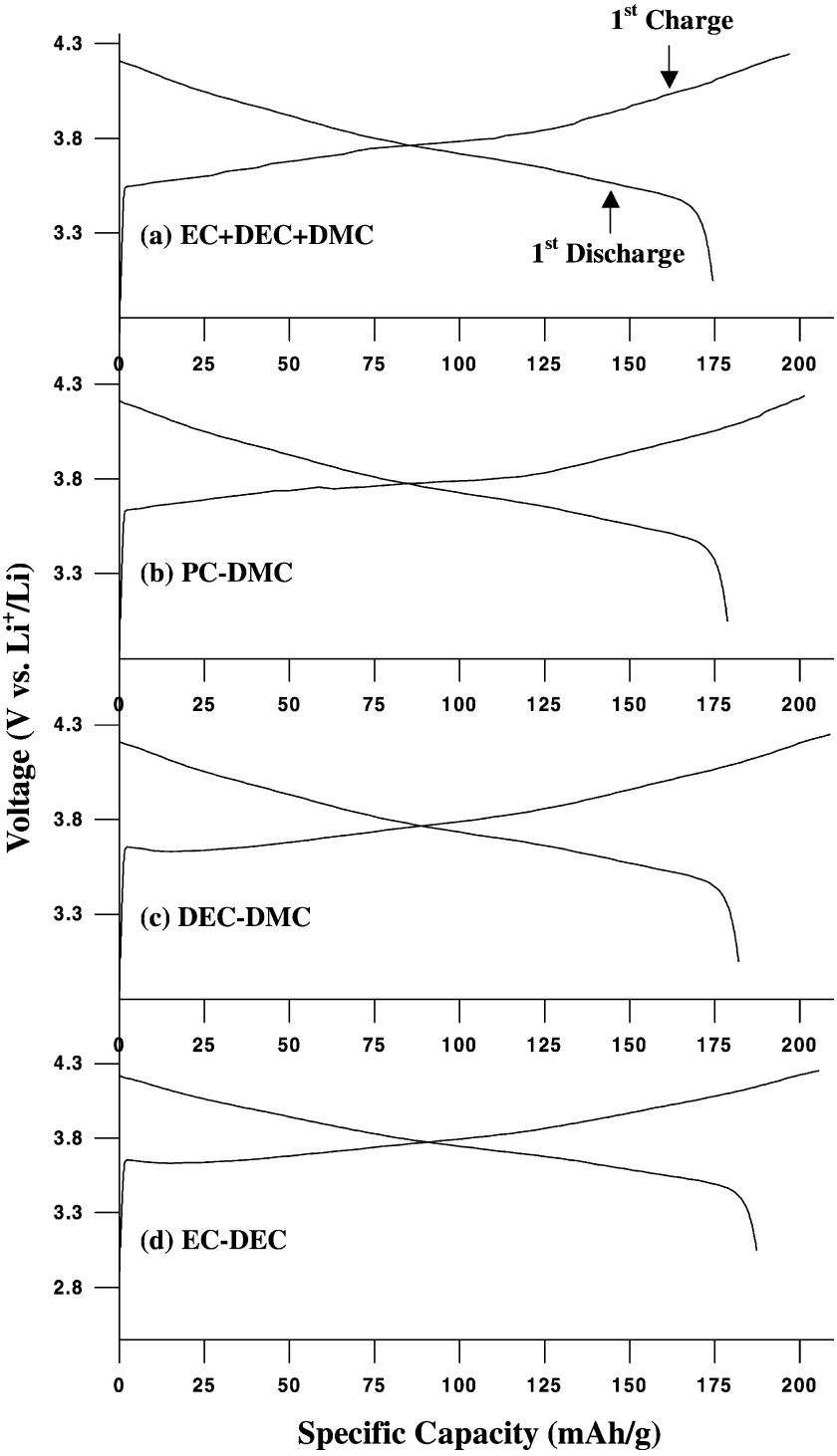

Fig. 1. Charge–discharge profiles of $Li_xNi_{0.8}Co_{0.2}O_2$ in different electrolytes: (a) 1 M $LiPF_6$ in EC:DEC:DMC (35:15:50); (b) 1 M $LiPF_6$ in PC:DMC (50:50); (c) 1 M $LiPF_6$ in DEC:DMC (50:50); (d) 1 M $LiPF_6$ in EC:DEC (50:50).

It is also possible that films formed on the surface of the cathode by the decomposition of the electrolyte could influence the interfacial resistance [31–33]. According to Aurbach et al. [34], the solid electrolyte interface formed on the surface of oxide cathodes in lithium cells influences the transport of lithium ions between the solution phase and the cathode active mass. In fact, Morita et al. [25] suggested that electrolyte composition influenced the performance of $LiNiO_2$ cathodes in terms of the kinetics of lithium diffusion through the electrode–electrolyte interface. The composition of such surface films will depend on the composition of the electrolyte. It is pertinent to note here that

ester exchange reactions between carbonate esters and products formed thereby can also influence the surface film composition, as has been noted with graphite anodes [35,36]. Some of the products of such ester exchange reactions can be rather weird. EC and DMC, for example, may react to yield a mixed carbonate such as dimethyl-2,5-dioxahexane carboxylate, $CH_3(OOC–O–CH_2–CH_2–O–COO)CH_3$ [36]. Thus, ester exchange reactions have the potential to drastically affect not only electrolyte properties, but also the kinetics of lithium intercalation and stability of the solid electrolyte interface [37].

3.2. Electrochemical impedance spectroscopic studies

The electrochemical reaction of a transition metal oxide electrode in a non-aqueous electrolyte involves many contributing processes such as the transport of lithium ions in the electrolyte, charge-transfer across the electrode–electrolyte interface, and diffusion of lithium in the solid oxide matrix [21,23,24]. The kinetic parameters associated with an electrode material can be understood from its a.c. impedance response. The Nyquist plots recorded for the $Li_xNi_{0.8}Co_{0.2}O_2$ electrode in different non-aqueous electrolytes are shown in Figs. 2–5. The Nyquist plots were recorded at different charge and discharge states namely, partially charged (3.8 V), fully charged (4.2 V), partially discharged (3.8 V) and fully discharged (∼3.4 V) states. The impedance plots recorded for the as-assembled cells showed a large high-frequency depressed semicircle and a low-frequency tail. The high-frequency semicircle is associated with the surface film on the cathode, while the Warburg tail implies that the electrode processes under this condition are controlled by diffusion. This behavior was seen in all the systems studied regardless of the electrolyte used. However, in their Nyquist plots for the as-assembled cells with $LiNiO_2$, Morita et al. [26] observed only the linear part, which they simply ascribed to diffusion processes at the interface.

As lithium was deintercalated, the size of the high-frequency semicircle decreased, only to increase when lithium was re-intercalated. The plots also show an additional semicircle in the medium frequency region. The presence of two semicircles indicates well-separated lithium insertion steps with different time constants. The high-frequency semicircle, as noted above, represents the impedance due to a surface film on the oxide electrode surface, while the other semicircle is related to a slow charge transfer process at the interface, as well as a capacitance at the film/bulk oxide interface. A simultaneous shifting of the medium-frequency semicircle towards the origin as the deintercalation proceeded can also be seen. This is attributed to an increase in the electronic conductivity of the oxide material as it turned from a semiconductor to a metallic conductor as progressively more lithium was removed from it [21]. Several groups have reported similar observations [21–24]. Morita et al. [25,26] and Choi et al. [38] reported a dip in the impedance of Li_xNiO_2 for x values between 0.4 and 0.8, which they ascribed to changes in the interlayer distance in the crystal lattice [25] and to the concentration of lithium and electron density on the surface of the oxide [38]. The second semicircle in the highly charged states is also accompanied by a large Warburg impedance component. The high-frequency features, which reflect the lithium ion migration properties across the surface films, cannot be deciphered at the beginning of the charging process because the scales are too large (Figs. 4 and 5). The high-frequency regions are, therefore, shown expanded in Figs. 4c and 5c.

As can be seen from the figures, the solution resistance, R_e, does not show much dependence on the voltage at which the impedance spectra were recorded. Levi et al. [22] reported similar results for thin $Li_xNi_{0.8}Co_{0.2}O_2$ electrodes at different values of x during charge and discharge. Since the cell reaction is independent of the electrolyte, changes in the lithium activity of the electrodes should have no effect on the electrolyte composition. The capacity values calculated were in the order of μF.

In our study, the impedance spectra recorded in the partially charged and partially discharged conditions show three distinct semicircles and a low-frequency tail. The well-defined high-frequency semicircle is associated with the surface film on the oxide electrode, the medium-frequency semicircle with the charge transfer processes across the solid electrode–electrolyte interface, and the low-frequency semicircle with the electron kinetics in the solid matrix. The low-frequency tail, a Warburg type, is attributed to the diffusion of lithium ions in the solid matrix. The analysis of such electrochemical processes can be very involved, but can conveniently be interpreted with equivalent circuit models.

Cells cycled 10 times were also subjected to impedance measurements in their completely discharged states in order to understand surface changes on the oxide cathode brought about by interaction with the electrolytes during repeated charging and discharging (Fig. 6). A comparison of Fig. 6 with Figs. 2–5 shows that the impedances of the surface films, as reflected by the high-frequency semicircles, were much lower than those obtained with the as-assembled cells. It is possible that the compact, high-resistance Li_2CO_3 film on the pristine surface gets incorporated with other reaction products of the oxide and with the electrolyte components to form a less resistant, and possibly less compact film. Our observations agree with those of previous researchers [19].

The equivalent circuit models used in the present study involve a combination of resistances (R), constant phase elements (Q), represented as CPEs in the circuit diagrams, and Warburg impedance, as shown in Fig. 7. The number of 'RQ' elements in series used in an equivalent circuit depends on the number of semicircles present in the Nyquist plot measured at each voltage. The impedance parameters associated with the Nyquist plots recorded at the different voltages in the different electrolytes were determined. The typical values obtained with 1 M $LiPF_6$ in 50:50 EC:DEC are presented in Table 1. Levi et al. [22] in their

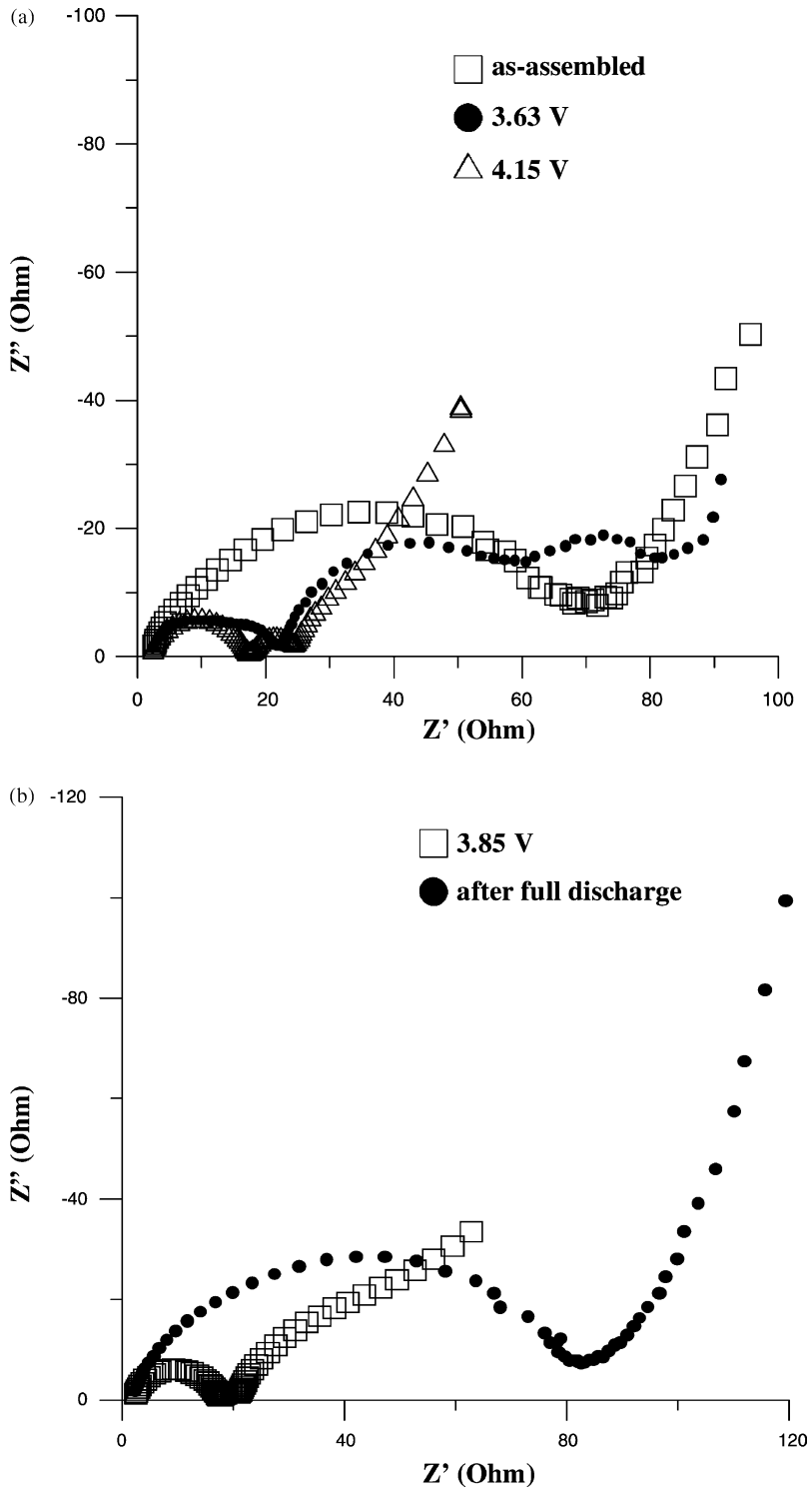

Fig. 2. Impedance spectra of $Li_xNi_{0.8}Co_{0.2}O_2$ in 1 M $LiPF_6$ in EC:DEC (50:50): (a) charging; (b) discharging.

studies on thin $Li_xNi_{0.8}Co_{0.2}O_2$ electrodes used a model comprised of a combination of resistances and capacitances ascribed to the surface film and the charge transfer processes. However, the electronic resistances were not considered [23]. Nobili et al. [24], on the other hand, interpreted their results by incorporating electronic resistance components with the usual parameters associated with surface film, charge-transfer and diffusion in the solid matrix. In our models below, we have included contributions from the electronic resistances.

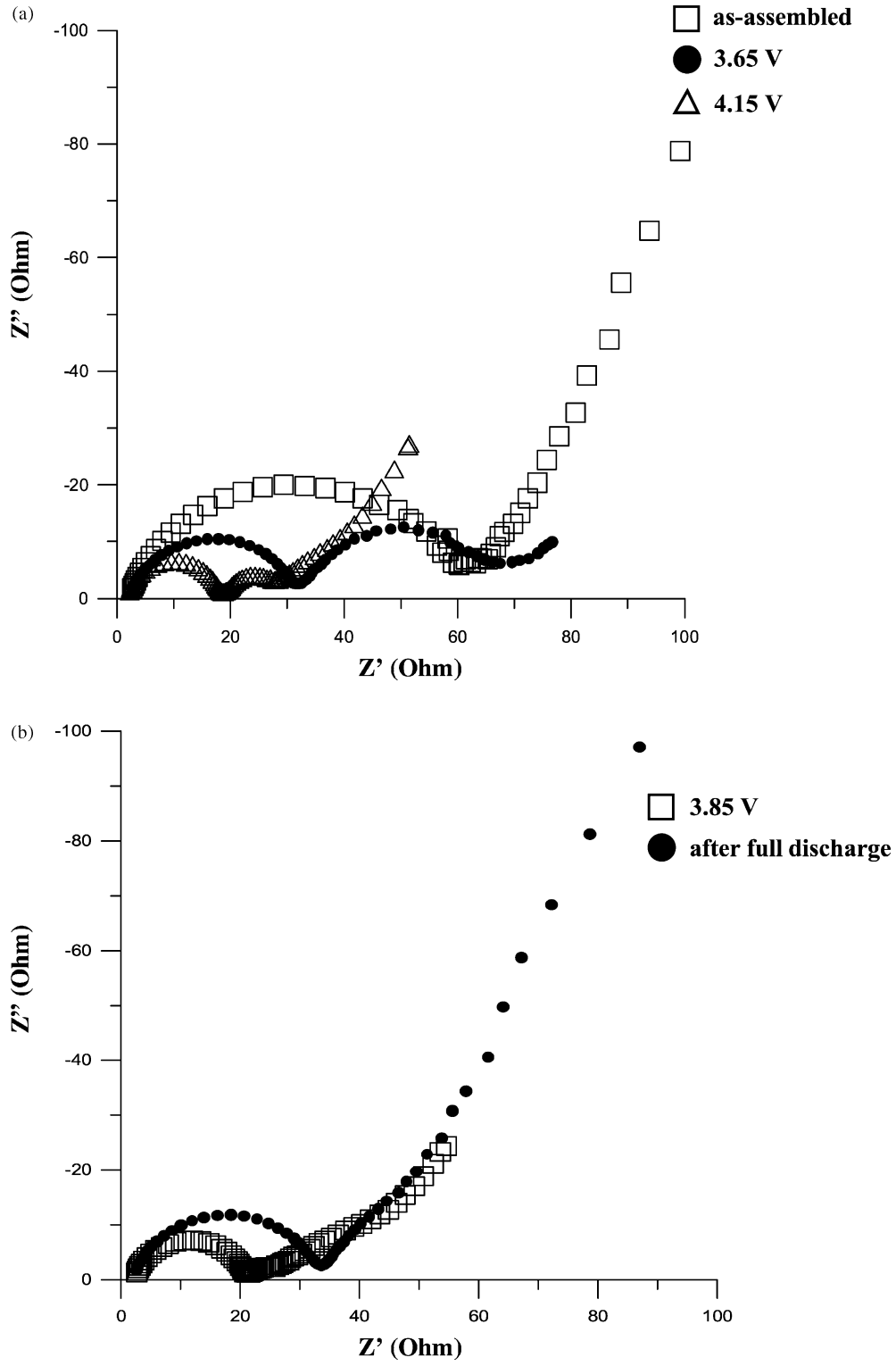

Fig. 3. Impedance spectra of $Li_xNi_{0.8}Co_{0.2}O_2$ in 1 M $LiPF_6$ in DEC:DMC (50:50): (a) charging; (b) discharging.

Our Model A has a solution resistance R_e, a constant phase element (CPE) Q, a resistance in parallel and a Warburg impedance. In Model B, there are two CPEs and charge transfer resistance R_{ct}, in parallel, as shown in Fig. 7, corresponding to the number of semicircles in the impedance plots. The number of semicircles depends on the voltage at which the impedance spectra are recorded. The Nyquist plots recorded for the as-assembled cells (i.e. at $x = 1$ in $Li_xNi_{0.8}Co_{0.2}O_2$) were fitted according to Model A, irrespective of the electrolyte used. The impedance plots

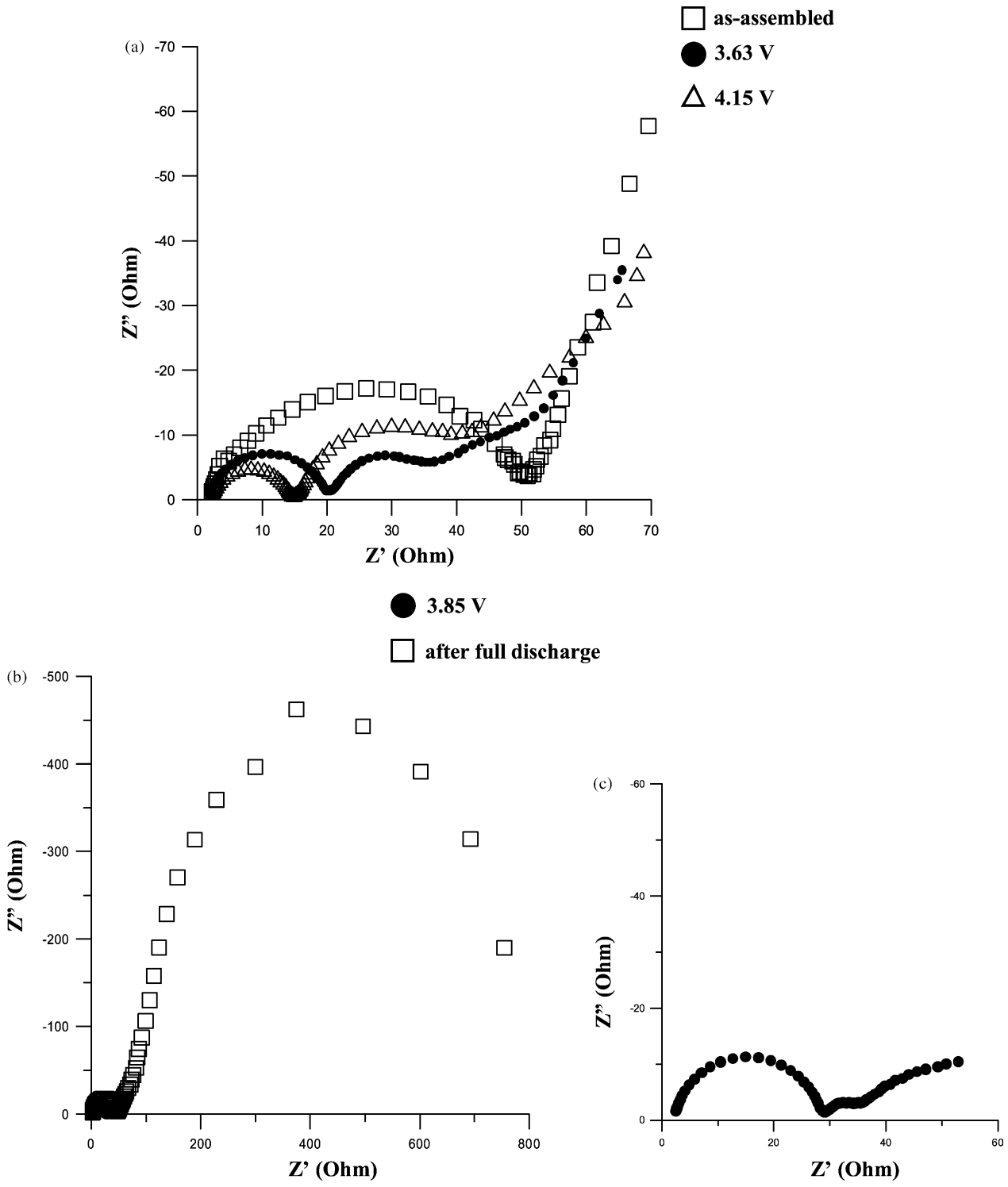

Fig. 4. Impedance spectra of $Li_xNi_{0.8}Co_{0.2}O_2$ in 1 M $LiPF_6$ in PC:DMC (50:50): (a) charging; (b) discharging; (c) expanded view of the impedance spectrum recorded at 3.85 V during discharge.

of cathodes charged to a voltage between 3.7 and 3.8 V showed three semicircles, and were assigned to Model C. The additional low-frequency semicircle is attributed to the contribution from the electronic resistance [24]. For the fully charged cathode (4.2 V), the impedance plot comprised of a well-defined high-frequency semicircle, a medium-frequency semicircle and a Warburg impedance. The above behavior was explained based on Model B. The systems reverted to their original impedance responses after complete discharge to 3.0 V for all the electrolyte

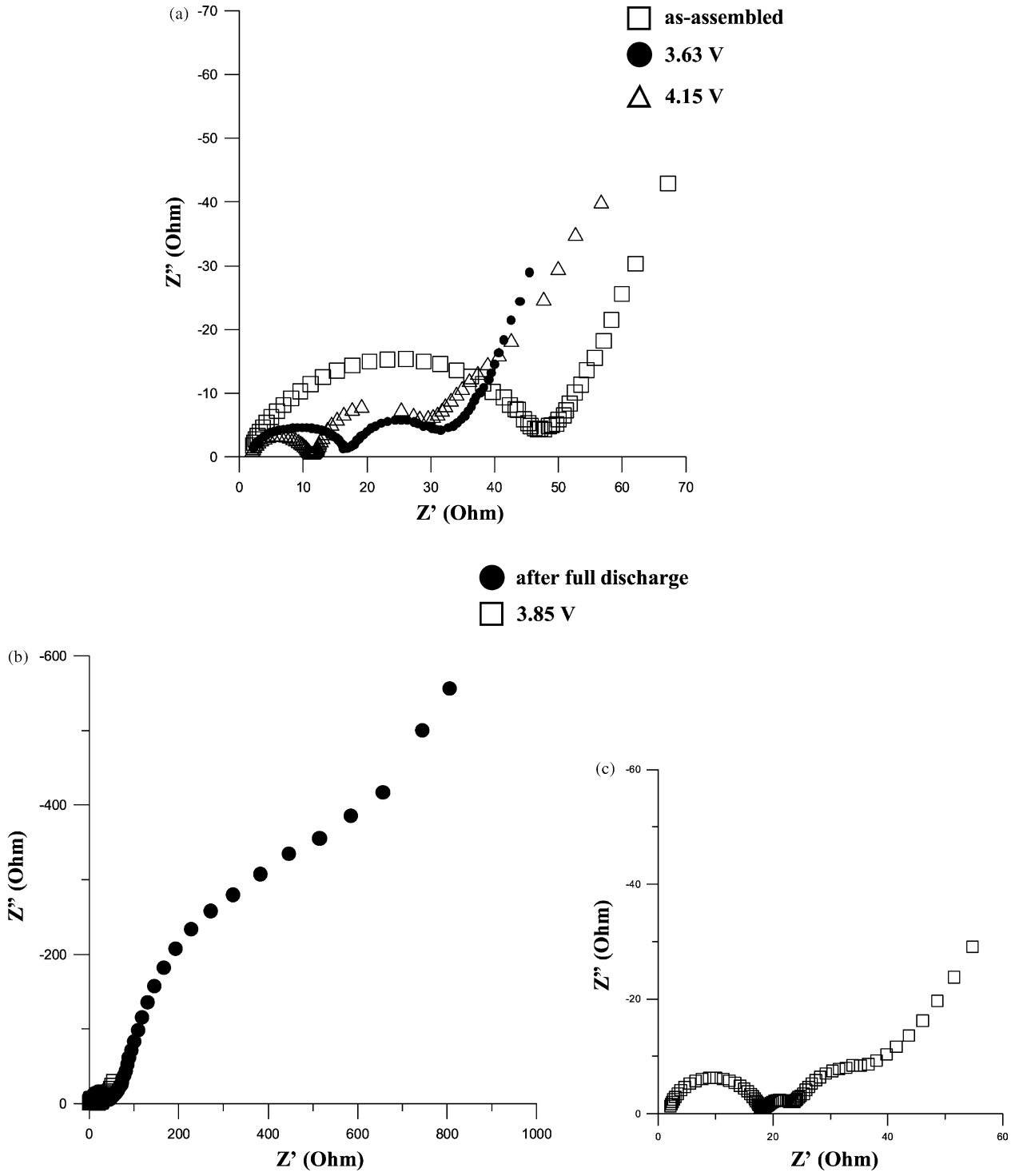

Fig. 5. Impedance spectra of $Li_xNi_{0.8}Co_{0.2}O_2$ in 1 M $LiPF_6$ in EC:DEC:DMC (35:15:50): (a) charging; (b) discharging; (c) expanded view of the impedance spectrum recorded at 3.85 V during discharge.

solutions studied, except for the one with an EC:DEC:DMC combination as the solvent. The reason for this peculiar behavior is not clear. The charge transfer resistances were of the order of a few ohms, as shown in Table 1. In the present impedance plot, there was no clear Warburg tail. The impedance spectra for the cycled cells (after seven charge–discharge cycles) also showed a similar enlarged second semicircle, masking the Warburg impedance [18].

Comparing the impedance parameters derived from the proposed equivalent circuits, the solution resistance seems to be almost independent of the voltage at which the impedance

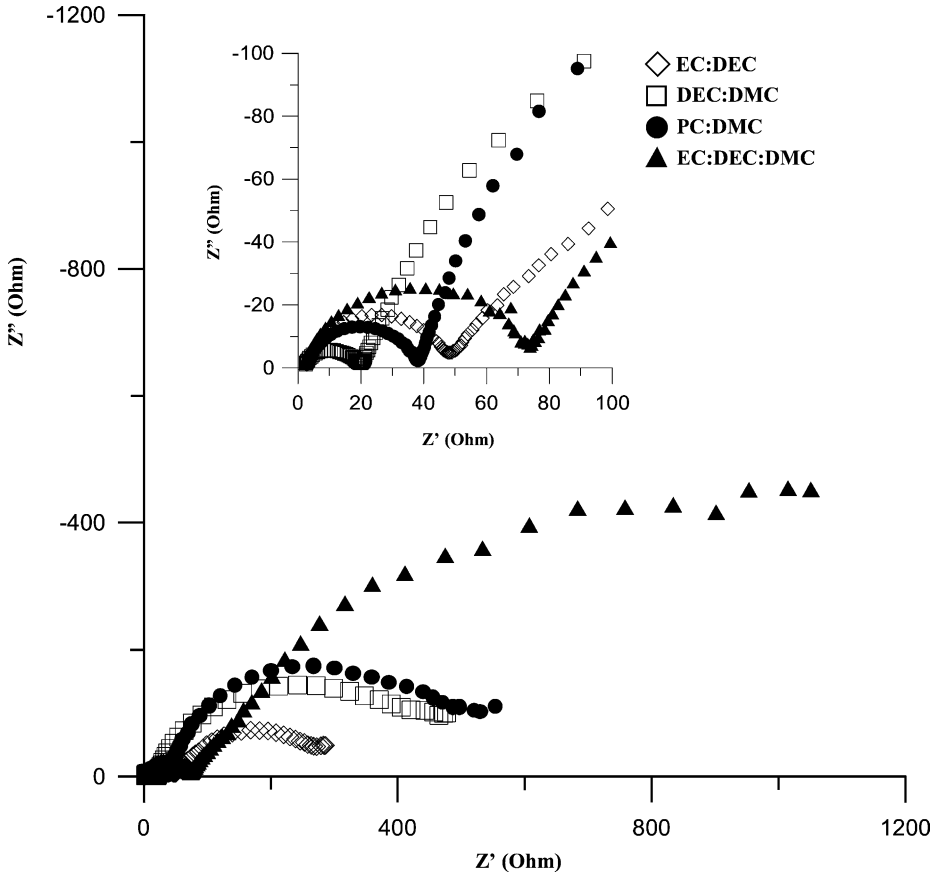

Fig. 6. Impedance spectra of $Li_xNi_{0.8}Co_{0.2}O_2$ after 10 cycles in different electrolytes. The high-frequency region is shown expanded in the inset.

spectra were recorded. Thus, the solution resistance was independent of the state-of-charge of the cathodes. There was also no appreciable change in the impedance parameters with a change in the composition of the electrolyte. However, in a similar study on a $LiNiO_2$ electrode in different organic electrolytes, where both salts and solvents were varied, the electrode/solution interfacial resistance was found to be slightly dependent on the salt used in the electrolyte [25,26]. On the other hand, we found that the charge transfer resistance varied with the voltage at which the impedance spectrum was recorded. As can be seen from Table 1, R_{ct} decreased with an increase in the deintercalation level. Our results are in agreement with several others reported for transition metal oxides [19,21–24]. The capacitance associated with the second semicircle in the medium-frequency range is due to the charge transfer reaction and the associated double layer capacitance at the electrode–electrolyte interface. The capacitance values for the charge transfer process were of the order of 10–20 mF cm^{-2} for all the systems studied here at all intercalation–deintercalation voltages. The large capacitance values can be related to the porous structure and morphology of the cathode particles. Our values for the capacitance agree with those of Levi et al. [19].

Table 1
Impedance parameters for $Li_xNi_{0.8}Co_{0.2}O_2$ in 1 M $LiPF_6$ in EC:DEC (50:50)

Voltage	R_e (Ω)	R_p (Ω)	R_{ct} (Ω)	CPE-1		CPE-2		R3 (Ω)	CPE-3		Z_w Warburg impedance		
				T	P	T	P		T	P	W1-R	W1-T	W1-P
As-assembled (OCV, 3.2 V)	1.42	–	69.00	3.536E−5	0.73	–	–				78.16	0.85	0.41
3.63 V (charging)	1.49	20.00	36.07	6.622E−5	0.69	0.0230	0.88	8.34	3.235	1.35	75.00	680.00	0.46
4.15 V (charging)	2.17	14.74	7.31	7.248E−6	0.89	0.0287	0.75	–	–	–	238.50	2207.00	0.61
3.85 V (discharging)	2.17	14.81	3.33	6.551E−6	0.90	0.0124	0.77	–	0.350	1.01	150.00	2300.00	0.38
After full discharge (OCV, 3.4 V)	1.40	–	81.50	1.810E−5	0.76	–	–	–	–	–	45.00	0.75	0.43

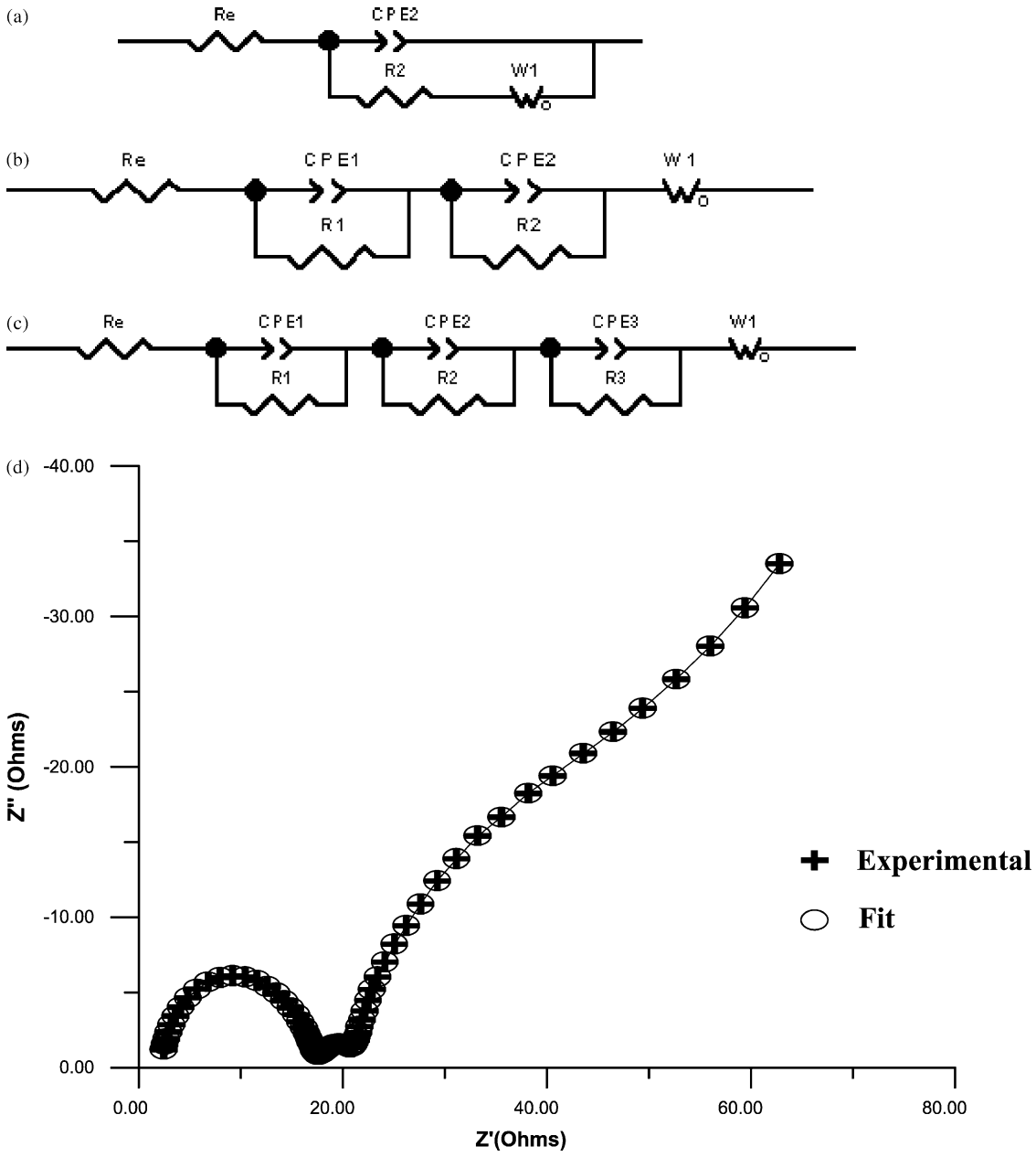

Fig. 7. Equivalent circuit models proposed to explain the impedance behavior of $Li_xNi_{0.8}Co_{0.2}O_2$ in different electrolyte systems: (a) Model A; (b) Model B; (c) Model C; (d) a typical fit of experimental impedance data using Model C.

4. Conclusions

Electrochemical impedance spectroscopy was employed to understand the electrode kinetics at the $Li_xNi_{0.8}Co_{0.2}O_2$ electrode. Capacity of the synthesized material was evaluated by galvanostatic charge–discharge cycling. $LiPF_6$ solutions (1 M) in mixed carbonate solvents such as EC:DEC, DEC:DMC, PC:DMC and EC:DEC:DMC were used as the electrolytes. The Nyquist plots exhibited semicircles corresponding to the surface film, the charge transfer across the electrode–electrolyte interface and electron reaction kinetics, and a Warburg impedance spike corresponding to lithium diffusion in the oxide electrode. The solution resistances of the systems were found to be independent of both the lithium content x, in $Li_xNi_{0.8}Co_{0.2}O_2$ and the electrolyte used. However, the charge transfer resistance was found to be dependent on x. The semicircles tended to shift towards the origin as the deintercalation proceeded.

Equivalent circuit models were proposed to explain the complicated impedance spectra at the various intercalation and deintercalation levels. The capacitance values calculated from the impedance plots were found to agree well with those reported. In general, the impedance response of the system was found to be independent of the electrolyte

composition. However, the electrolyte had a definite effect on the charge–discharge behavior of the cathode material. Coin cells with 1 M $LiPF_6$ in EC:DEC (1:1 by volume) delivered the highest capacity and the best cyclability. With this electrolyte, the first-cycle capacity was 187 mAh g^{-1}, while the first-cycle capacities obtained with the other electrolytes were between 174 and 182 mAh g^{-1}.

Acknowledgements

Financial support for this work from the National Science Council of the Republic of China [NSC-90-2214-E-008-003] is gratefully acknowledged. TPK thanks the National Science Council for the award of a post-doctoral fellowship.

References

[1] B. Scrosati, Nature 373 (1993) 557.
[2] P. Barboux, J.M. Tarascon, F.K. Shokoohi, J. Solid State Chem. 94 (1991) 185.
[3] J. Morales, C. Perez-Vicente, J.L. Tirado, Mater. Res. Bull. 25 (1990) 623.
[4] A. Rougier, I. Saadoune, P. Gravereau, P. Willmann, C. Delmas, Solid State Ionics 90 (1996) 83.
[5] B.J. Neudecker, R.A. Zuhr, B.S. Kwak, J.B. Bates, J. Electrochem. Soc. 145 (1998) 4161.
[6] T. Ohzuku, A. Ueda, M. Nagayama, J. Electrochem. Soc. 140 (1993) 1862.
[7] W. Li, J.N. Reimers, J.R. Dahn, Solid State Ionics 67 (1993) 123.
[8] T. Ohzuku, A. Ueda, M. Kouguchi, J. Electrochem. Soc. 142 (1995) 4033.
[9] J.N. Reimers, E. Rossen, C.D. Jones, J.R. Dahn, Solid State Ionics 61 (1993) 335.
[10] H. Arai, S. Okada, Y. Sakurai, J. Yamaki, J. Electrochem. Soc. 144 (1997) 3117.
[11] B.V.R. Chowdari, G.V. Subba Rao, S.Y. Chow, Solid State Ionics 140 (2001) 55.
[12] I. Saadoune, C. Delmas, J. Mater. Chem. 6 (1996) 193.
[13] W. Li, J. Curie, J. Electrochem. Soc. 144 (1997) 1773.
[14] C. Delmas, M. Menetrier, L. Croguennec, I. Saadoune, A. Rougier, C. Pouillerie, G. Prado, M. Grune, L. Fournes, Electrochim. Acta 45 (1999) 243.
[15] J. Cho, H. Jung, Y. Park, G. Kim, H.S. Lim, J. Electrochem. Soc. 147 (2000) 15.
[16] C. Delmas, I. Saadoune, A. Rougier, J. Power Sources 43–44 (1993) 595.
[17] J. Aragane, K. Matsui, H. Andoh, S. Suzuki, F. Fukuda, H. Ikeya, K. Kitaba, R. Ishikawa, J. Power Sources 68 (1997) 13.
[18] J. Fan, P.S. Fedkiw, J. Power Sources 72 (1998) 165.
[19] M.D. Levi, G. Salitra, B. Markovsky, H. Teller, D. Aurbach, U. Heider, L. Heider, J. Electrochem. Soc. 146 (1999) 1279.
[20] K. Dokko, M. Mohamedi, Y. Fujita, T. Itoh, M. Nishizawa, M. Umeda, I. Uchida, J. Electrochem. Soc. 148 (2001) A422.
[21] F. Croce, F. Nobili, A. Deptula, W. Lada, R. Tossici, A. D'Epifanio, B. Scrosati, R. Marassi, Electrochem. Commun. 1 (1999) 605.
[22] M.D. Levi, K. Gamolky, D. Aurbach, U. Heider, R. Oesten, Electrochim. Acta 45 (2000) 1781.
[23] F. Nobili, F. Croce, B. Scrosati, R. Marassi, Chem. Mater. 13 (2001) 1642.
[24] F. Nobili, R. Tossici, F. Croce, B. Scrosati, R. Marassi, J. Power Sources 94 (2001) 238.
[25] O. Yamada, M. Ishikawa, M. Morita, Electrochim. Acta 45 (1999) 1607.
[26] M. Morita, O. Yamada, M. Ishikawa, J. Power Sources 81–82 (1999) 425.
[27] G.T.K. Fey, R.F. Shiu, V. Subramanian, J.G. Chen, C.L. Chen, J. Power Sources 103 (2002) 265.
[28] J.M. Tarascon, D. Guyomard, Solid State Ionics 69 (1994) 293.
[29] D. Guyomard, J.M. Tarascon, J. Power Sources 54 (1995) 92.
[30] Z.X. Shu, I.J. Davidson, R.S. McMillan, J.J. Murray, J. Power Sources 68 (1997) 618.
[31] J.G. Thevenin, R.H. Muller, J. Electrochem. Soc. 134 (1987) 273.
[32] M. Morita, S. Aoki, Y. Matsuda, Electrochim. Acta 37 (1992) 119.
[33] K. Kanamura, S. Toriyama, S. Shiraishi, Z. Takehara, J. Electrochem. Soc. 143 (1996) 2548.
[34] D. Aurbach, M.D. Levi, E. Levi, G. Salitra, B. Markovsky, H. Teller, J. Electrochem. Soc. 145 (1998) 3024.
[35] G.E. Blomgren, J. Power Sources 81–82 (1999) 112.
[36] U. Heider, R. Oesten, M. Jungnitz, J. Power Sources 81–82 (1999) 119.
[37] R. Yazami, M. Deschamps, S. Genies, J.C. Frison, J. Power Sources 68 (1997) 110.
[38] Y.M. Choi, S.I. Pyun, J.S. Bae, S.I. Moon, J. Power Sources 56 (1995) 25.